Direct Torque Control of Permanent Magnet Synchronous Motor With Reduced Torque Ripple and Commutation Frequency

Yongchang Zhang, *Member, IEEE*, and Jianguo Zhu, *Senior Member, IEEE*

***Abstract*—In conventional direct torque controlled (DTC) permanent magnet synchronous motor drive, there is usually undesired torque and flux ripple. The existing literature have proposed some methods to reduce torque and flux ripple by optimizing the duty ratio of the active vector. However, these methods are usually complicated and parameter dependent. This paper first compares the performances of three duty determination methods in detail and then proposes a very simple but effective method to obtain the duty ratio. The novel method is superior to the existing methods in terms of simplicity and robustness. By appropriately arranging the sequence of the vectors, the commutation frequency is reduced effectively without performance degradation. To further improve the performance of system, a low-pass filter-based voltage model with compensations of amplitude and phase is employed to acquire accurate stator flux estimation. The proposed scheme is able to reduce the torque and flux ripple significantly while maintaining the simplicity and robustness of conventional DTC at the most. Simulations and presented experimental results validate the effectiveness of the proposed schemes in this paper.**

***Index Terms*—AC motor drives, low-pass filters (LPFs), permanent magnet synchronous motor (PMSM) drives, ripple reduction, torque control.**

I. Introduction

FIELD-ORIENTED control (FOC) and direct torque control (DTC) are the two most popular methods for high performance ac drives [1]. Compared to FOC, DTC can provide extremely high dynamic response with very simple structure, i.e., no need of rotary coordinate transformation, inner current regulator, or pulsewidth modulation (PWM) block [1]–[4]. Because of the merits of the earlier, recently DTC has been extended from conventional induction motor (IM) drive to permanent magnet synchronous motor (PMSM) drive [5], [6]. However, conventional DTC employs two hysteresis comparators and a heuristic switching table to obtain quick dynamic response, which causes undesired torque and flux ripple, variable switching frequency, and acoustic noises.

In the past decades, numerous schemes have been proposed to address these problems of conventional DTC. Many of them [4]–[12] employ space vector modulation (SVM) to produce continuous voltage vectors, which can adjust the torque and flux more accurately and moderately, hence the torque and flux ripples were reduced while obtaining fixed switching frequency. Another merit of using SVM is that the sampling frequency does not need to be as high as that in conventional DTC. Various methods are proposed to obtain the commanding voltage vector, including deadbeat control [10], sliding mode control [8], PI controller [9], etc. In the SVM-based DTC schemes, rotary coordinate transformation is often needed [5]–[12], which is more computationally intensive than the conventional DTC [13].

Another category of modified DTC does not need the SVM block and all the calculations were implemented in stationary coordinate, hence preserving the merits of conventional DTC. Multilevel inverter was introduced to obtain more voltage vectors [14], [15]; however, the hardware cost and system complexity are increased. For two level inverter, more voltage vectors can be synthesized by dividing one sampling period into several intervals [1], thus a more accurate and complex switching table can be constructed. In [1], the divided intervals are equal and only for vector synthesis purpose. In other literature [16]–[19], the intervals are obtained based on certain optimizations, differing in duration numbers. According to the principle of obtaining the time durations, they can be classified as: analytical calculation based on torque ripple minimization [16], [17], equalizing the torque with the reference value over one cycle [18] and fuzzy logic adaptation [19]. These methods [16]–[19] achieve excellent performance, but they are usually complicated and rely much on the knowledge of motor parameters.

Recently, predictive control was introduced to achieve high performance control [20]–[26]. This kind of method is similar to DTC only in that they both directly manipulate the final voltage vector. In [20], by evaluating the defined cost function of each possible switching states, the one best satisfying the performance requirement is selected. A three-level inverter-fed DTC motor drive is presented in [21], which utilizes a predictive horizon greater than one to obtain reduced switching frequency while keeping torque, flux, and neutral point potential within their respective hysteresis bands. Recently, the predictive torque control has also been applied in synchronous reluctance motor [27] and doubly fed IM [28].

The DTC requires the information of stator flux, which can be easily obtained from the voltage model by integrating the back electromotive force behind the stator resistance. However,

Manuscript received March 16, 2010; revised May 3, 2010 and June 13, 2010; accepted July 7, 2010. Date of current version December 27, 2010. Recommended for publication by Associate Editor J. O. Ojo.

The authors are with the Faculty of Engineering and Information Technology, University of Technology Sydney, NSW 2007, Australia (e-mail: yozhang@eng.uts.edu.au; joe@eng.uts.edu.au).

Color versions of one or more of the figures in this paper are available online at http://ieeexplore.ieee.org.

Digital Object Identifier 10.1109/TPEL.2010.2059047

in practical digital implementation, pure integration usually suffers from the dc drift and initial value [29]–[33]. To overcome the problems of pure integration, low-pass filter (LPF) was proposed to replace pure integration [29]. This causes errors in both magnitude and phase when the motor frequency is lower than the cutoff frequency, so compensation is necessary. The compensation method in [30] requires twice transformation and/or incorporation of PI, increasing the system complexity. Other method employs cascaded programmable LPF [31] to improve the accuracy of LPF; however, its dynamic performance is relatively poor [32] and the computation complexity is increased. In fact, the accuracy of LPF can be significantly improved by compensating the phase and amplitude errors [33] directly, which is simple and will be employed in this paper to provide accurate stator flux estimation. There are also other kinds of flux estimators or observers based on the model of machine [34]. By introducing the feedback of current errors, the observers present better robustness, accuracy, and dynamic performance. However, they are very complex and negates the merits of simplicity in DTC, so they are not discussed here.

In this paper, after comparing three kinds of methods of obtaining the duty ratio of the active vector, a simple yet effective method will be proposed to decrease the complexity and eliminate the parameter dependence while achieving excellent performance. All calculations are implemented in stationary frame and no rotary coordinate transformation is needed, hence preserving the simplicity of conventional DTC. The commutation frequency can be reduced effectively by appropriately arranging the vector sequence during one cycle while maintaining the performance of torque and flux. An LPF-based voltage model with compensation is used to obtain accurate stator flux estimation, which only requires the knowledge of stator resistance and can be easily implemented. It is the aim of this paper to reduce the torque and flux ripple and commutation frequency while preserving the structure simplicity as much as possible. The proposed scheme is simulated and experimentally verified on a two-level inverter-fed PMSM drive.

II. Model of PMSM

A. Machine Equations

For PMSM, the model in rotor synchronous coordinate is the most popular, because all the parameters become constant. The machine equations of a PMSM in synchronous frame are expressed as follows (the components indicated by dq)

$$u_d = R_s i_d + \frac{d\psi_d}{dt} - \omega\psi_q \tag{1}$$

$$u_q = R_s i_q + \frac{d\psi_q}{dt} + \omega\psi_d \tag{2}$$

$$\psi_d = L_d i_d + \psi_f \tag{3}$$

$$\psi_q = L_q i_q \tag{4}$$

where

R_s	stator resistance
$L_d,\ L_q$	d-axis and q-axis inductance
ψ_f	permanent magnet flux
$\psi_d,\ \psi_q$	d-axis and q-axis stator flux
$u_d,\ u_q$	d-axis and q-axis stator voltage
$i_d,\ i_q$	d-axis and q-axis stator current
ω	electrical rotor speed

and the torque is expressed as

$$T_e = \frac{3}{2}p\left(\psi_d i_q - \psi_q i_d\right) \tag{5}$$

where p is the number of pole pairs.

For the DTC PMSM drive, stationary frame is preferred to avoid complex rotary coordinate transformation. By translating the machine equations from synchronous dq coordinate to stationary $\alpha\beta$ coordinate, we get

$$u_\alpha = R_s i_\alpha + \frac{d\psi_\alpha}{dt} \tag{6}$$

$$u_\beta = R_s i_\beta + \frac{d\psi_\beta}{dt} \tag{7}$$

$$\psi_\alpha = L_\alpha i_\alpha + L_{\alpha\beta} i_\beta + \psi_f \cos\theta_e \tag{8}$$

$$\psi_\beta = L_{\alpha\beta} i_\alpha + L_\beta i_\beta + \psi_f \sin\theta_e \tag{9}$$

where $L_\alpha = \Sigma L + \Delta L\cos 2\theta_e$, $L_\beta = \Sigma L - \Delta L\cos 2\theta_e$, $L_{\alpha\beta} = \Delta L \sin 2\theta_e$, $\Sigma L = (L_d + L_q)/2$, $\Delta L = (L_d - L_q)/2$, and θ_e is the electrical rotor angle. It is seen that the expressions of inductance are complex.

This can be further simplified if surface-mounted PMSM (SPMSM) is addressed, where the d-axis and q-axis inductance are equal to synchronous inductance L_s, i.e., $L_d = L_q = L_s$. In that case, the SPMSM equations can be expressed using complex vectors as

$$\boldsymbol{u_s} = R_s \boldsymbol{i_s} + \frac{d\boldsymbol{\psi_s}}{dt} \tag{10}$$

$$\boldsymbol{\psi_s} = L_s \boldsymbol{i_s} + \boldsymbol{\psi_r} \tag{11}$$

where $\boldsymbol{\psi_r} = \psi_f e^{j\theta_e}$ and the torque in stationary frame is expressed as

$$T_e = \frac{3}{2}p\boldsymbol{\psi_s} \otimes \boldsymbol{i_s} = \frac{3}{2}p\left(\psi_\alpha i_\beta - \psi_\beta i_\alpha\right). \tag{12}$$

B. Effects of Voltage on Torque

For voltage source inverter-fed DTC, the voltage vector is the sole controllable input variable, so it is desirable to analytically derive the relationship between the torque and voltage vector. From (10) and (11), we can get

$$L_s\frac{d\boldsymbol{i_s}}{dt} = \boldsymbol{u_s} - R_s\boldsymbol{i_s} - j\omega\boldsymbol{\psi_r}. \tag{13}$$

From (12), the torque differentiation with respect to time t is

$$\frac{dT_e}{dt} = \frac{3}{2}p\left(\frac{d\boldsymbol{\psi_s}}{dt} \otimes \boldsymbol{i_s} + \frac{d\boldsymbol{i_s}}{dt} \otimes \boldsymbol{\psi_s}\right). \tag{14}$$

Substitute (10), (11), and (13) into (14) and omit the tedious derivation process, the final torque differentiation is

$$\begin{aligned} L_s\frac{dT_e}{dt} &= -R_s T_e - \frac{3}{2}p\omega\boldsymbol{\psi_r} \odot \boldsymbol{\psi_s} + \frac{3}{2}p\boldsymbol{\psi_r} \otimes \boldsymbol{u_s} \\ &= \Delta T_{e1} + \Delta T_{e2} + \Delta T_{e3}. \end{aligned} \tag{15}$$

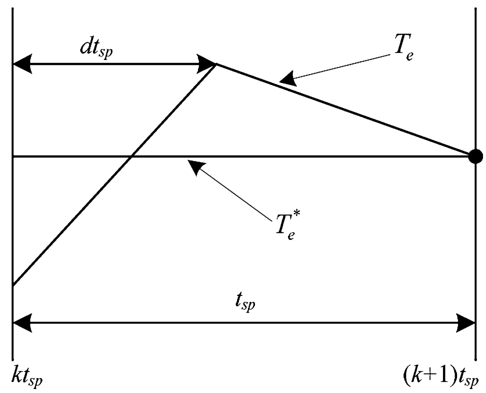

Fig. 1. Method I of duty decision.

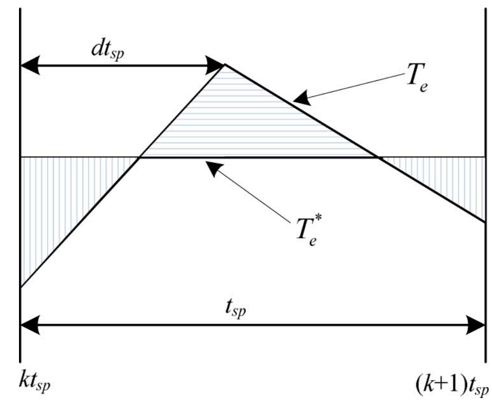

Fig. 2. Method II of duty decision.

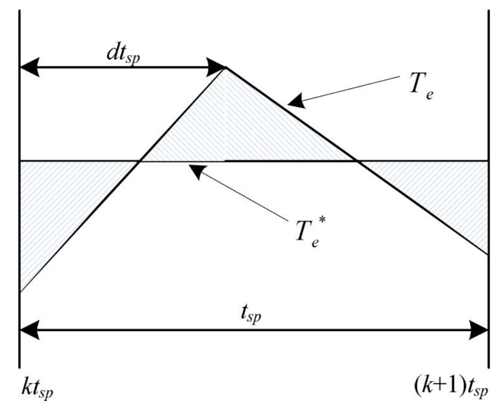

Fig. 3. Method III of duty decision.

It is seen from (15) that the torque differentiation is composed of three parts, just similar to the case in IM [16]. The first part ΔT_{e1} is always negative with respect to T_e; the second part is also negative and proportional to rotor speed; the last term is the positive one and it reflects the effect of stator voltage on T_e. When zero voltage vector is selected, the torque differentiation becomes

$$L_s \frac{dT_e}{dt} = -R_s T_e - \frac{3}{2} p\omega \boldsymbol{\psi_r} \odot \boldsymbol{\psi_s} \tag{16}$$

so the zero voltage vector always decreases the torque.

In conventional DTC, the hysteresis comparator fails to differentiate the amplitude of flux and torque errors, and the vector selected from the switching table works during the whole period. In many cases, it is not necessary for the selected vector to work for the entire period to meet the performance requirement of torque and flux, and this is the main reason for large torque ripple. By introducing zero vector during one sampling period, the effects of voltage on torque can be adjusted to be more moderate, hence diminishing the ripples in torque.

III. Overview of Duty Ratio Determination Methods

A. Basic Principle

From (15), it is seen that the torque can be changed by adjusting the amplitude and time duration of $\boldsymbol{u_s}$. The amplitude is decided by the dc bus voltage and is usually fixed, while the time duration of $\boldsymbol{u_s}$ can be varied from zero to the whole period, which is equivalent to changing the voltage vector length. The null vector only decreases the torque, as shown in (16), while appropriate nonzero vector can increase the torque, so it is possible to employ both zero vector and nonzero vector during one cycle to reduce the torque ripple. In this paper, the appropriate nonzero vector is also referred as "active vector." The key point is how to decide the time duration of the two vectors, or the duty ratio of the active vector.

B. Classical Duty Determination Methods

There are three classical methods to determine the duty ratio, as illustrated in Figs. 1–3, which were initially developed for IM DTC drive.

The method I aims to make the instantaneous torque equal with the reference value at the end of the cycle, acting in a deadbeat fashion. This concept was originally developed in [35] in stationary coordinate and then revisited in synchronous stator flux coordinate in [10]. A quadratic equation has to be solved to find the optimal duty in [35] and the result is complex. In this paper, a simplified deadbeat control is proposed, which mainly focuses on the torque. The principle of method I can be expressed as

$$T_e(k+1) = T_e^*. \tag{17}$$

It is the aim of method II to make the mean torque equal to the reference value over the entire cycle, as shown in (18). This kind of method is called direct mean torque control in [18] and [36].

$$\frac{1}{t_{\rm sp}} \int_{kt_{\rm sp}}^{(k+1)t_{\rm sp}} (T_e - T_e^*)\, dt = 0. \tag{18}$$

The method III aims to make the torque ripple RMS value over one cycle to be minimal [16], and the principle is expressed as

$$\frac{1}{t_{\rm sp}} \int_{kt_{\rm sp}}^{(k+1)t_{\rm sp}} (T_e - T_e^*)^2\, dt \to \min. \tag{19}$$

Suppose the rising slope s_1 and falling slope s_2 of the instantaneous torque are known for the active vector and null vector, which are indicated by (15) and (16), respectively. During a small sampling period $t_{\rm sp}$, slopes s_1 and s_2 can be considered to be constant because the dynamics of flux and speed are not fast [16]. Under this assumption, the time duration of the active vector for the three kinds of methods can be obtained by solving the (17) to (19) as

$$d_1 t_{\rm sp} = \frac{T_e^* - T_0 - s_2 t_{\rm sp}}{s_1 - s_2} \tag{20}$$

$$d_2 t_{\rm sp} = t_{\rm sp} - \sqrt{\frac{t_{\rm sp}}{s_1 - s_2}\left(2\left(T_0 - T_e^*\right) + s_1 t_{\rm sp}\right)} \tag{21}$$

$$d_3 t_{\rm sp} = \frac{2\left(T_e^* - T_0\right) - s_2 t_{\rm sp}}{2 s_1 - s_2} \tag{22}$$

where T_0 indicates the initial torque value at kth sampling instant; d_1, d_2, and d_3 are the duty ratios of the active vector for method I, II, and III, respectively.

C. In-Depth Analysis and Consideration of the Existing Methods

The three duty determination methods in (20)–(22) have very different forms; however, they are all reported to have better performance when compared to conventional DTC, validating the fact the torque ripple in DTC can be reduced effectively by introducing zero voltage vector. Apart from the analytical methods, these is another method, which uses fuzzy logic adaptive method to obtain the duty ratio, as introduced in [19]. It is also reported in [19] that the torque ripple is reduced effectively when compared to classical DTC. The various forms of analytical methods in (20)–(22) and the fuzzy logic based method in [19] enlighten people to consider that it may not be very important how the duty determination is obtained, but the important matter is that zero vector should be ensured.

Although there are various methods in obtaining the duty ratio, so far no comparative study of these methods in terms of torque ripple has been reported. Also, the influence of motor parameter mismatch was not investigated in the literature. It would be interesting to evaluate the performances of these methods comparatively.

IV. Proposed DTC Scheme

A. Principle of Proposed Duty Determination Method

The prior arts in (20)–(22) are complicated and parameter dependent. To eliminate these drawbacks, it is desirable to develop a method, which is simple to implement and robust to parameter variations while reducing the torque ripple. The diversity in the duty expression enlightens us that the parameter-dependent coefficients in (20)–(22) may be eliminated by keeping them constant without significantly degrading the performance of torque ripple reduction. Otherwise, it is not easy to explain how can all various methods achieve reduced torque ripple irrespective of the specific duty expression. In other word, the fact that using zero vector can reduce the torque ripple has been widely acknowledged, but there seems no unified answer to the duty determination. In this paper, a novel method to obtain the duty ratio will be proposed, which eliminates the complexity and parameter dependence as in (20)–(22).

Before giving the novel duty determination method, let us first revisit the duty in (20), which can be rewritten as

$$d_1 = \frac{T_e^* - T_0 - s_2 t_{\rm sp}}{(s_1 - s_2) t_{\rm sp}} = \frac{T_e^* - T_0}{(s_1 - s_2) t_{\rm sp}} + \frac{-s_2}{s_1 - s_2}. \tag{23}$$

The first term in (23) is proportional to the torque error and the second term is proportional to the falling slope s_2 of torque. To eliminate the parameter dependence, we can assume that the denominator $(s_1 - s_2)t_{\rm sp}$ is constant. However, the second term in (23) related to s_2 is still very complex and parameter dependent, as indicated by (16). Notice that falling slope s_2 of torque is caused by a null vector, which is responsible for the decrease in stator flux, it would be natural to make the second term proportional to flux error. Considering the fact that the duty is nonnegative, the final expression of the devised parameter-independent duty ratio is

$$d = \left|\frac{E_T}{C_T}\right| + \left|\frac{E_\psi}{C_\psi}\right| = \left|\frac{T_e^* - T_0}{C_T}\right| + \left|\frac{\psi_s^* - \psi_0}{C_\psi}\right| \tag{24}$$

where T_e^* and ψ_s^* are the reference values for torque and stator flux, respectively; ψ_0 is the stator flux at the kth sampling instant; and C_T and C_ψ are two positive constants. By using fixed constants for C_T and C_ψ, it is expected that the novel method will be less affected by the disturbances in calculating the torque slope. The tuning of C_T and C_ψ is a tradeoff between dynamic response and steady-state performance. Larger value of C_T and C_ψ will produce less torque and flux ripples, but the dynamic performance is degraded. Extensive simulation and experimental results tell that permanent flux and half-rated torque provides a good starting point for C_ψ and C_T to achieve good compromise between steady and dynamic performance. Nevertheless, it is found that the variations of them do not cause significant difference in the system performance, as shown in Section VII.

B. Theoretical Analysis and Comparison With Other Methods

Simplicity is the first merit of the proposed method when compared to prior methods. It is seen that (24) is much simpler than those in (20)–(22), requiring only twice sums and multiplications. On the contrary, the equations in (20)–(22) are obtained through analytical methods, which are complex in expressions and computational intensive, even requiring square root function in (21).

Robustness against motor parameter mismatch is the second merit of the proposed method. For the prior arts in (20)–(22), the torque slope shown in (15) and (16) are needed to fulfill the duty determination, which requires the information of stator resistance, d-axis and q-axis inductance, PM flux and rotor position. For the proposed method, no additional motor parameters are needed to obtain the duty ratio, so it should be less affected by the variations in motor parameters than other methods.

Apart from the motor parameter robustness, the proposed method is less affected by the one-step digital delay than other methods. It is well known that in practical digital implementation, the voltage vector is usually applied during the next period, i.e., the voltage is decided at kth sampling instant, but it is not applied until the $(k+1)$ th sampling instant [20], [23], [24]. To eliminate this delay, the torque and flux at $(k+1)$ th sampling instant should be employed to decide the active vector, which will be subsequently used to calculate the torque slope and then the duty ratio in prior arts. For conventional DTC, by compensating the one-step delay, better performance in terms of torque and flux ripples as well as increased commutation frequency can be obtained. For the novel method, the influence of one-step delay is similar to that in conventional DTC, because only stator flux and torque are involved in the implementation. For prior arts, the influence of one-step delay is more serious, because the active vector is employed in the calculation of torque slope, which will affect the duty ratio implementation. In the early literature of [18] for method II in (21), the torque slope is obtained by using the value at the last cycle, which does not compensate the one-step delay, and it is reported that this algorithm is best suited for lower speed. In this paper, it will be shown by compensating the one-step delay, better performance can be obtained for prior arts.

The fourth merit of the proposed method is that it is insensitive to the exchange in the switching sequence of active vector and null vector. In the prior arts in (20)–(22), it is assumed that the active vector will be applied first followed by the null vector. However, this limitation does not exist in the proposed method, because the duty ratio is not binding to the vector switching sequence. The possible benefit from the exchange in switching sequence is that the commutation frequency can be reduced, which leads to a decrease in switching losses. This issue will be studied in this paper for the novel method in (24) as well as prior arts in (20)–(22).

Regarding steady performance in terms of torque and flux ripples, it is not easy to give a direct comparison between the proposed method and prior arts. Furthermore, it may be not even possible for the direct comparison among the prior arts, even if they are analytically obtained. The main difficulty comes from the initial torque T_0 in (20)–(22), which increases the complexity when substituting the duty ratios into the expression of torque ripple. Even if method III aims to minimize the torque ripple during one cycle, it may not be easy to assert that method III will surely present the lowest torque ripple among these methods, because T_0 is unknown, not to mention considering other factors, such as one-step delay in digital implementation. It seems that the comparisons of these methods in terms of toque ripple reduction may be only achieved through computer simulation and experimental validation. In this paper, these methods will be comparatively investigated through simulations, and a comprehensive conclusion is drawn to summarize the results.

V. Stator Flux Estimation

In DTC, the voltage model in (10) is preferred because it requires less parameters than the current model. In practical digital implementation, the pure integration in (10) is sensitive to dc drift in the input. A very natural method is incorporating a high-pass filter (HPF) behind the pure integrator. This is equivalent to an LPF. Although the introduction of HPF eliminates the dc drift, it brings errors in both magnitude and phase. The phase error between the pure integrator and LPF in steady state of sine waveform is

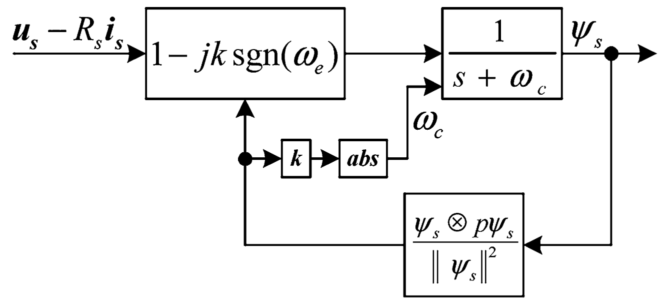

Fig. 4. LPF with compensation.

$$\Delta\theta = \arctan\frac{\omega_e}{\omega_c} - \frac{\pi}{2} = -\arctan\frac{\omega_c}{\omega_e} \tag{25}$$

and the amplitude error is

$$\Delta G = \frac{\sqrt{\omega_e^2 + \omega_c^2}}{\omega_e} \tag{26}$$

where ω_e is the synchronous frequency of stator flux and ω_c is the cutoff frequency of the LPF. To eliminate the steady-state errors caused by the LPF, a compensation term is needed, i.e.,

$$G = \Delta G \times e^{\Delta\theta} = \frac{\sqrt{\omega_e^2 + \omega_c^2}}{\omega_e} e^{-\arctan\frac{\omega_c}{\omega_e}} = 1 + \frac{\omega_c}{j\omega_e}. \tag{27}$$

The cutoff frequency ω_c should be selected carefully, because big error will be produced when the motor frequency is lower than the cutoff frequency. However, very low cutoff frequency will degrade the effectiveness of eliminating the dc component. It is better to set the cutoff frequency proportional to the synchronous frequency ω_e, i.e., $\omega_c = k\omega_e$. The typical range of k is between 0.1 and 0.5 [33]. The synchronous frequency ω_e can be calculated from the stator flux vector as

$$\omega_e = \frac{\boldsymbol{\psi_s} \otimes p\boldsymbol{\psi_s}}{\|\boldsymbol{\psi_s}\|^2} = \frac{\psi_\alpha\left(u_\beta - R_s i_\beta\right) - \psi_\beta\left(u_\alpha - R_s i_\alpha\right)}{\psi_\alpha^2 + \psi_\beta^2}. \tag{28}$$

The whole diagram of the LPF with compensation is illustrated in Fig. 4. The compensation is carried out before the LPF component to improve the dynamic performance [33]. The effectiveness of the LPF-based voltage model with compensation is illustrated in Fig. 5, where the motor is started from standstill to 1000 r/m. It is seen that the LPF with compensation exhibits excellent performances in both dynamic response and steady-state accuracy.

VI. Comparative Study of Duty Determination Methods

So far, no comparative study of the various duty determination methods have been reported in the literature. In this section, the three classical methods and the proposed methods will be comparatively investigated using MATLAB/Simulink from four aspects: steady response without commutation frequency reduction, steady response with commutation frequency

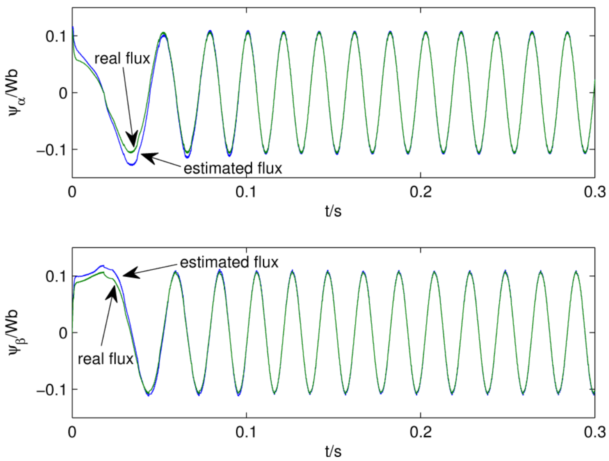

Fig. 5. Stator flux estimation using LPF with compensation.

TABLE I
MOTOR AND SYSTEM PARAMETERS

Number of pole pairs	p	3
Permanent magnet flux	ψ_f	0.1057 Wb
Stator resistance	R_s	1.8Ω
d-axis and q-axis inductance	L_d, L_q	15 mH
Rated speed	n_N	2000 rpm
Rated torque	T_N	4.5 Nm
Rated line-line voltage	U_N	128 V
DC bus voltage	U_{dc}	200 V
Sampling period	t_{sp}	100 μs
Torque constant gain	C_T	2 Nm
Flux constant gain	C_ψ	0.1 Wb
Stator flux reference	ψ_s^*	0.12 Wb

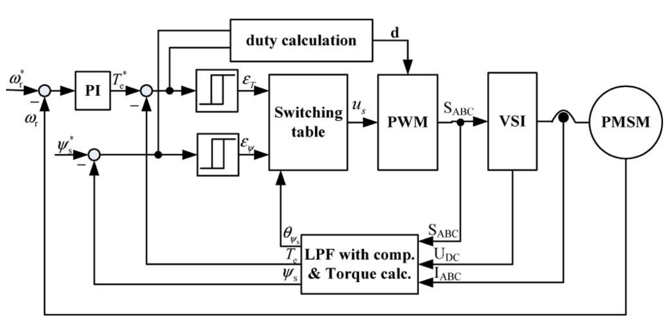

Fig. 6. Block diagram of proposed DTC.

reduction, steady response with one-step delay, and steady response with motor parameter mismatches. All results are obtained from one operation point of 1000 r/m (50% rated speed) without load. The sampling frequency is 10 kHz for all the methods, unless explicitly indicated. The parameters of motor and control system are listed in Table I. The system diagram for the duty-based DTC is illustrated in Fig. 6.

A. Implementation for the Duty-Based DTC

The implementation process is the same for methods I–III and the proposed method. The only difference is in the duty-determination methods, i.e., how the duty is obtained, which has been indicated in (20), (21), (22), and (24). The whole process can be simplified as three stages: active vector selection, duty determination, and vector output. The active vector is selected from the conventional DTC switching table in [37]. The signs of flux and torque error, ε_ψ and ε_T, are obtained from the hysteresis comparators with zero bandwidth. After obtaining the active vector and its duty ratio, the final output vectors in the next cycle are determined. The whole implementation process can be described as follows.

1) The active voltage vector is selected from the switching table in conventional DTC according to the signs of torque and flux errors.
2) For the proposed method, the duty ratio can be obtained directly from (24). For other methods, the rising slope s_1 and s_2 should be first calculated using (15) and (16), and then the duty can be obtained from (20) to (22).
3) In normal cases, the active vector will be first applied over the duration decided by (20), (21), (22), and (24) and then switched to the appropriate null vector for the rest time of the period. The appropriate null vector means that vectors "100," "010," and "001" will be followed by "000," while other vectors followed by "111." If the commutation frequency reduction is considered, the sequence of the active vector and the null vector will be decided by the switching state of the vector at the end of the last cycle. For example, if the vectors during the last cycle are "100" and "000" with "000" at the end, and the vectors to be applied in the next cycle are "001" and "000," in that case, "000" instead of "001" will be applied first to decrease the commutation frequency.
4) The duty ratio calculated from (20), (21), (22), and (24) should not be higher than 1, otherwise the active vector should be applied during the whole period. For method I to III, the duty calculated from (20) to (22) may also be negative. In the early paper [16], it is suggested that only the active vector be applied, because the torque is not in the steady state. However, the negative duty normally means the active vector is undesirable. In that case, the null vector should be more appropriate. The improvement in steady state by using null vector in the case of negative duty for method I to III has been verified by simulations and is adopted in this paper.
5) At the next cycle, the earlier process is repeated.

B. Steady Response Without Commutation Frequency Reduction

First, the steady response in terms of torque and flux ripples without considering commutation frequency reduction will be presented, i.e., in all methods, active vector will always be applied first followed by the appropriate null vector. Figs. 7–9 present the steady responses for conventional DTC, method I and II, method III, and the proposed method, respectively. From top to bottom, the curves shown in Figs. 7–9 are the duty ratios of the active vector, stator flux, and torque. It is seen that if no delay is considered, the commutation frequency of the basic DTC is comparable with other methods, but its torque ripple is much bigger than others. Best performance in terms of flux ripple can be observed for the proposed method, while the lowest

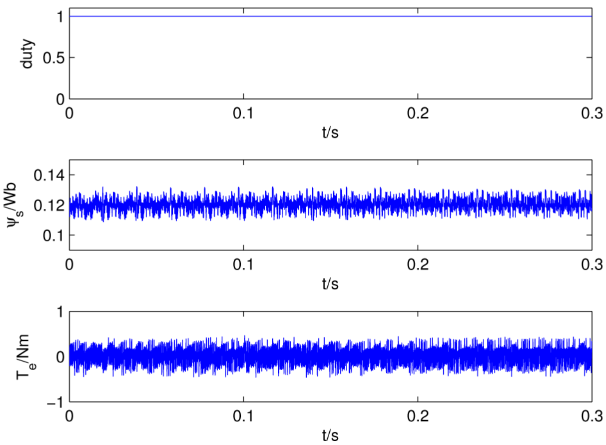

Fig. 7. Steady response of duty, stator flux, and torque for conventional DTC.

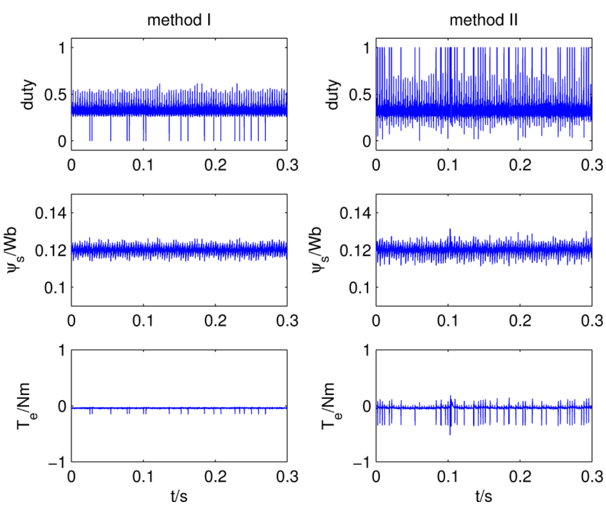

Fig. 8. Steady response of duty, stator flux, and torque for method I and II.

torque ripple is achieved by method III followed by method I and II. The torque ripple of the proposed method is relatively large when compared to other duty methods. There are irregular oscillations in the duties of method I to III, which is caused by the calculation of torque slope. On the contrary, the oscillation in the duty of the proposed method is very small and regular, which benefits from the constant value of C_T and C_ψ. Similar conclusions are obtained when changing the operation point with or without load. Due to the limit of pages, they are not listed here.

The quantitative results in terms of torque ripple $T_{\rm rip}$, flux ripple $\psi_{\rm rip}$, and commutation frequency $f_{\rm av}$ are summarized in Table II. Torque and flux ripples are calculated using the following equations:

$$T_{\rm rip} = \sqrt{\frac{1}{N}\sum_{i=1}^{N}\left(T_e\left(i\right) - T_{\rm av}\right)^2} \tag{29}$$

$$\psi_{\rm rip} = \sqrt{\frac{1}{N}\sum_{i=1}^{N}\left(\psi_s\left(i\right) - \psi_{\rm av}\right)^2} \tag{30}$$

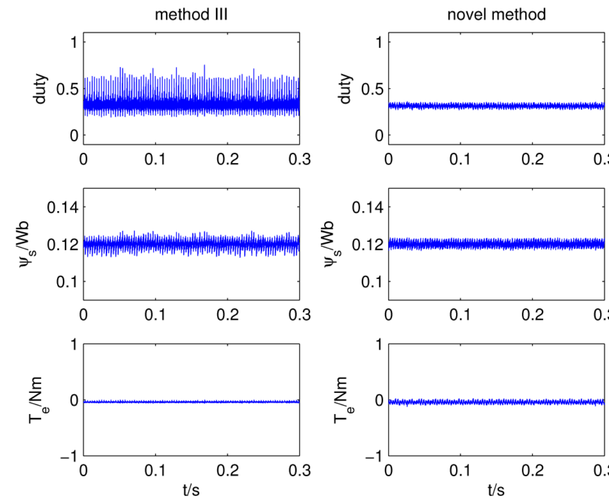

Fig. 9. Steady response of duty, stator flux, and torque for method III and novel method.

TABLE II
STEADY RESPONSES FOR VARIOUS METHODS

method	f_{av} (Hz)	ψ_{rip} (Wb)	T_{rip} (Nm)
basic DTC	7.45k	0.0048	0.2041
method I	8.43k	0.0023	0.0102
method II	8.26k	0.0030	0.0144
method III	8.37k	0.0026	0.0074
proposed method	8.59k	0.0015	0.0247

where N is the sampling number and $T_{\rm av}$ and $\psi_{\rm av}$ are the average value of torque and stator flux, respectively. The average commutation frequency $f_{\rm av}$ is calculated by counting the total commutation instants of a phase leg during a fixed period, e.g., 0.1 s in this paper.

C. Steady Response With Commutation Frequency Reduction

In this part, the steady responses for each method, considering the commutation frequency reduction introduced in the implementation part, are presented in Figs. 10 and 11. To obtain similar commutation frequency to other method, the result of the proposed method under 8 kHz sampling frequency is presented in Fig. 12. Table III summarizes the quantitative index of various methods. For the conventional DTC, there is no difference because only the nonzero vector is applied during one cycle. Under the condition of 10 kHz sampling frequency, the reductions in the commutation frequency are 35.11%, 28.21%, 27.48%, and 20.14% for method I, II, III, and the proposed method, respectively. There is very little difference in the flux ripples of all methods when compared to the prior results without commutation frequency reduction, but the torque ripples are much increased for method I–III. The proposed method still exhibits the lowest flux and duty ripples, and its torque ripple is now only larger than that of method III. Furthermore, it is seen from Fig. 12 that the performance of the proposed method is only slightly deteriorated when the sampling frequency is decreased from 10 to 8 kHz, showing strong robustness to the change in sampling frequency.

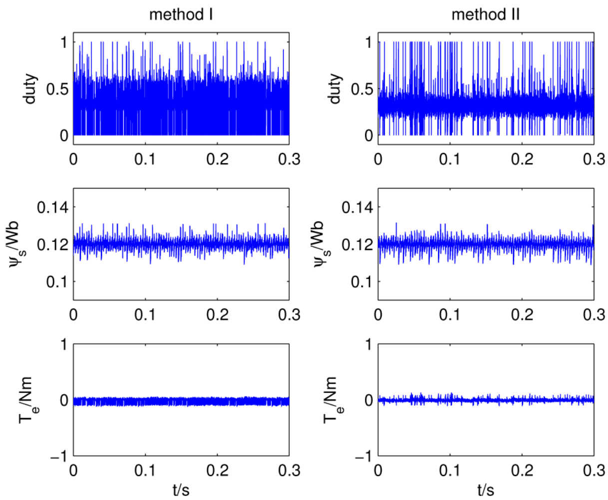

Fig. 10. Steady response of duty, stator flux, and torque for method I and II with reduced commutation frequency.

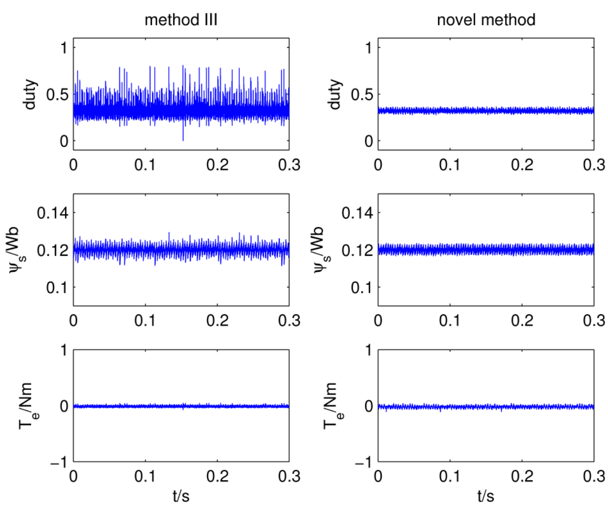

Fig. 11. Steady response of duty, stator flux, and torque for method III and the proposed method with reduced commutation frequency.

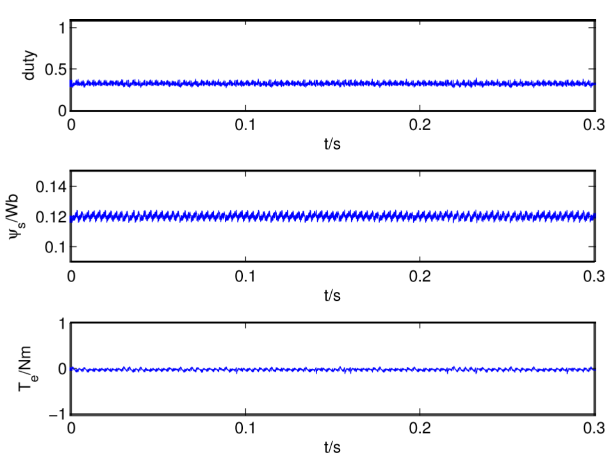

Fig. 12. Steady response of duty, stator flux, and torque for the proposed method with reduced commutation frequency (8 kHz sampling frequency).

TABLE III
STEADY RESPONSES WITH REDUCED COMMUTATION FREQUENCY

method	f_{av} (Hz)	ψ_{rip} (Wb)	T_{rip} (Nm)
basic DTC	7.45k	0.0048	0.2041
method I	5.47k	0.0031	0.0411
method II	5.93k	0.0034	0.0262
method III	6.07k	0.0026	0.0139
proposed method	6.86k	0.0015	0.0204
proposed method (f_s =8k Hz)	5.63k	0.0019	0.0226

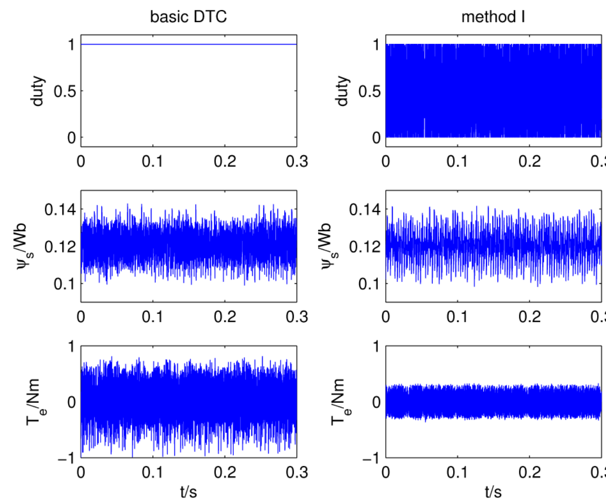

Fig. 13. Steady response of duty, stator flux, and torque for conventional DTC and method I with one-step delay.

D. Influence of One-Step Delay

The earlier results are obtained under the assumption of ideal condition, i.e., there is no one-step delay. In this section, we will compare the performance of each method under nonideal condition, i.e., with one-step delay caused by digital implementation.

Figs. 13–15 present the steady responses with one-step delay for conventional DTC and other duty-based methods. To achieve similar commutation frequency, the results of the proposed DTC under 7.5 kHz sampling frequency is also presented in Fig. 15. It is seen that for conventional DTC and method I–III, the torque and flux ripples are increased significantly when compared to the ideal cases in Figs. 7–9, which indicates that they suffer heavily from the one-step delay. There are large oscillations in the duty ratios of method I–III, although they still present better torque and flux performance than that of conventional DTC. On the contrary, the performance deterioration is insignificant for the proposed method in Fig. 15, exhibiting strong robustness. The quantitative index are shown in Table IV. With one-step delay, the average commutation frequency is also reduced significantly for basic DTC and method I–III, while the commutation frequency of the proposed method is only slightly reduced. The proposed method exhibits the best performances in terms of torque and flux ripple, even when the sampling frequency is decreased to 7.5 kHz.

Apart from the results with one-step delay, the performances of all methods considering commutation frequency reduction are also investigated, as shown in Figs. 16–17. To achieve similar commutation frequency, the result of the proposed method

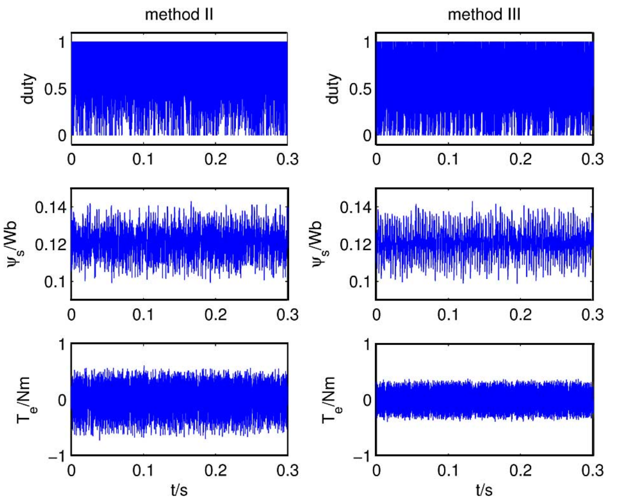

Fig. 14. Steady response of duty, stator flux, and torque for method II and III with one-step delay.

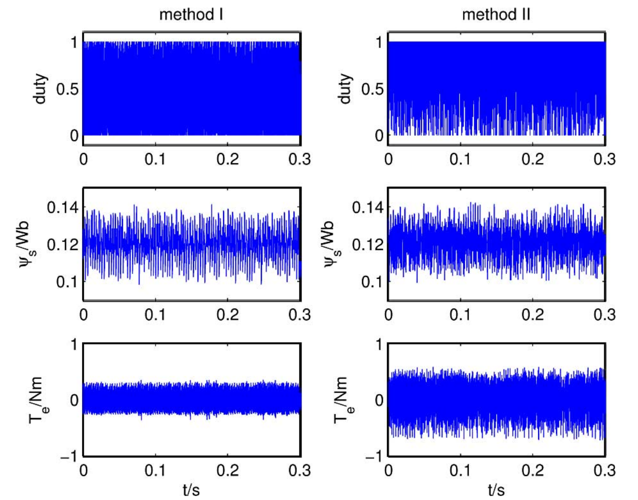

Fig. 16. Steady response of duty, stator flux, and torque for method I and II with one-step delay and commutation frequency reduction.

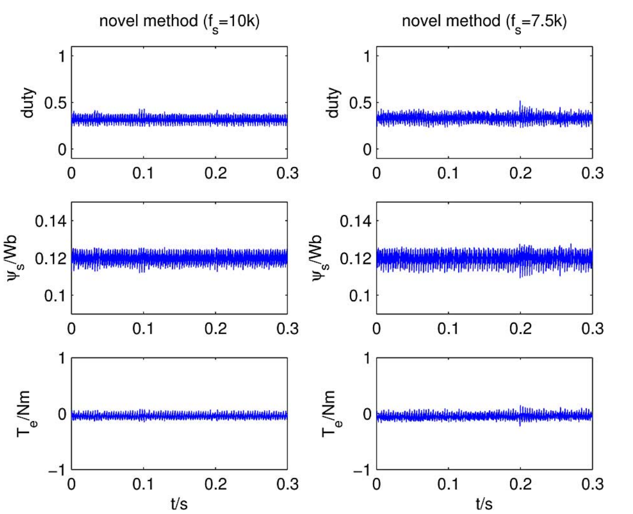

Fig. 15. Steady response of duty, stator flux, and torque for the proposed method with one-step delay and different sampling frequency.

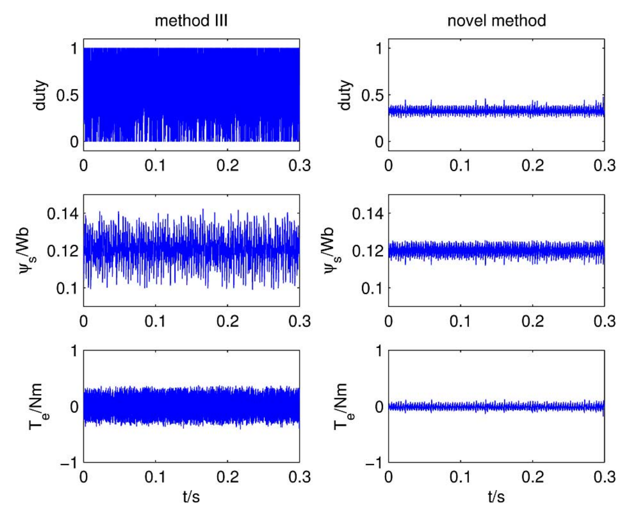

Fig. 17. Steady response of duty, stator flux, and torque for method III and the proposed method with one-step delay and commutation frequency reduction.

TABLE IV
STEADY RESPONSES WITH ONE-STEP DELAY

method	f_{av} (Hz)	ψ_{rip} (Wb)	T_{rip} (Nm)
basic DTC	3.02k	0.0083	0.3717
method I	5.36k	0.0087	0.1786
method II	3.93k	0.0085	0.3018
method III	5.85k	0.0082	0.2002
proposed method	7.50k	0.0027	0.0421
proposed method (f_s =7.5k Hz)	5.66k	0.0033	0.0535

TABLE V
STEADY RESPONSES WITH ONE-STEP DELAY AND REDUCED COMMUTATION FREQUENCY

method	f_{av} (Hz)	ψ_{rip} (Wb)	T_{rip} (Nm)
basic DTC	3.02k	0.0083	0.3717
method I	3.99k	0.0086	0.1732
method II	3.08k	0.0086	0.3100
method III	4.08k	0.0084	0.1982
proposed method	4.63k	0.0026	0.0403
proposed method (f_s =8k Hz)	3.82k	0.0034	0.0591

under 8 kHz sampling frequency is also presented in Fig. 18. The quantitative index for each method are summarized in Table V. It is seen that there is a further reduction in commutation frequency, while the performance deterioration is almost negligible for all the methods. Under the condition of 10 kHz sampling frequency, the reductions in the commutation frequency are 25.56%, 21.63%, 30.26%, and 38.27% for method I, II, III, and the proposed method, respectively, when compared to the results in Table IV. For the sake of improving efficiency, it is suggested using the scheme of commutation frequency reduction when one-step delay is not compensated for the duty-based DTC methods.

E. Robustness Against Motor Parameter Mismatch

The robustness against motor parameter variations is tested for the various methods, as shown in Figs. 19–21, where the stator resistance, inductance, and PM flux are all increased to 120%

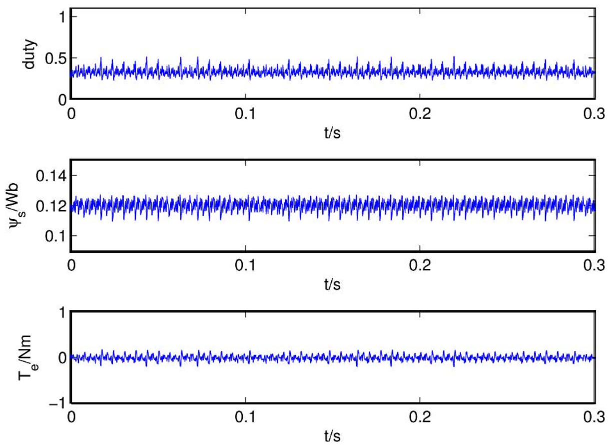

Fig. 18. Steady response of duty, stator flux, and torque for the proposed method with one-step delay and commutation frequency reduction (8 kHz sampling frequency).

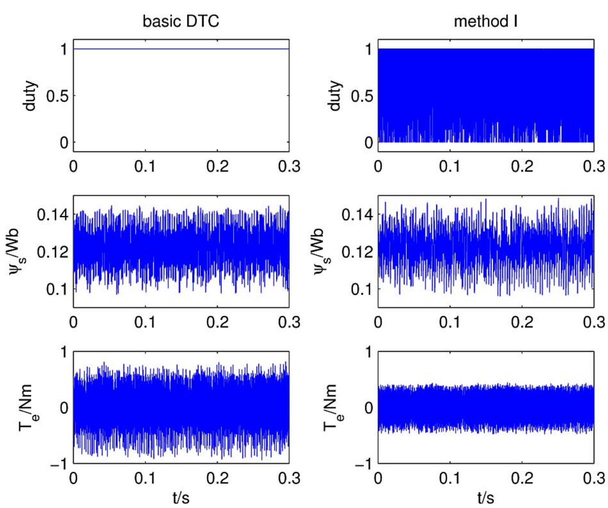

Fig. 19. Steady response of duty, stator flux, and torque for conventional DTC and method I with reduced commutation frequency and parameter mismatches.

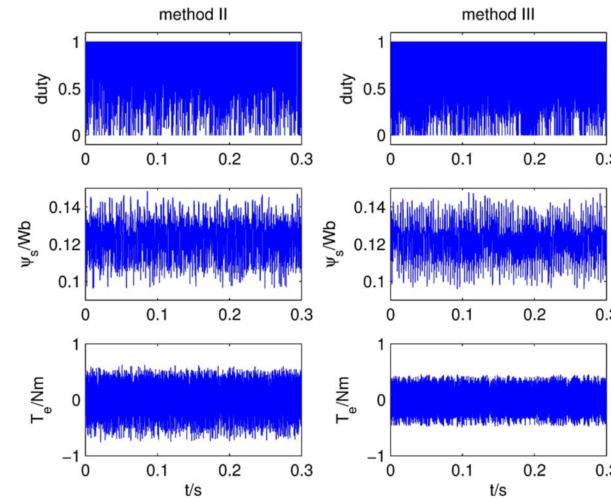

Fig. 20. Steady response of duty, stator flux, and torque for method II and III with reduced commutation frequency and parameter mismatches.

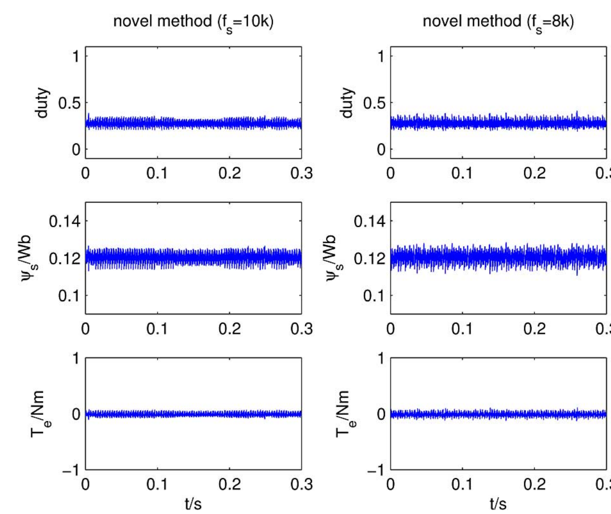

Fig. 21. Steady response of duty, stator flux, and torque for the proposed method with reduced commutation frequency and different sampling frequency.

of their respective nominal value. To achieve similar commutation frequency, the result of the proposed method under 8 kHz sampling frequency is also presented in Fig. 21. The one-step delay is not compensated and the commutation frequency reduction is considered for the tests. The simulation results reveal that the performance deterioration of method I–III is insignificant, except the flux ripple is increased. The torque ripple of the proposed method is even smaller than that without parameter mismatch in Table V. It can be said that each method shows strong robustness against motor parameter variations, especially for the proposed method. This is because the active vector is selected from the same switching table as basic DTC, which only considers the signs of torque and flux errors. The errors in amplitudes of torque and flux only affect the accuracy of duty determination. The results are summarized in Table VI. Similar results are observed for the ideal case without one-step delay, which is not listed here due to the page limitation.

TABLE VI
STEADY RESPONSES UNDER NONIDEAL CONDITION WITH REDUCED COMMUTATION FREQUENCY AND MOTOR PARAMETER MISMATCH

method	f_{av} (Hz)	ψ_{rip} (Wb)	T_{rip} (Nm)
basic DTC	3.28k	0.0102	0.3690
method I	3.93k	0.0105	0.2463
method II	3.13k	0.0105	0.3294
method III	3.91k	0.0098	0.2539
proposed method	4.73k	0.0027	0.0308
proposed method (f_s =8k Hz)	3.85k	0.0032	0.0375

F. Summary of the Comparative Study

From the results mentioned earlier, it is seen for conventional DTC, the torque and flux ripples can be reduced, and the commutation frequency is comparable with other methods by compensating one-step delay. For the proposed method, its merits can be summarized as: lowest flux and duty ripples in any case, even with decreased sampling frequency; lowest torque ripple under the condition of one-step delay; best robustness

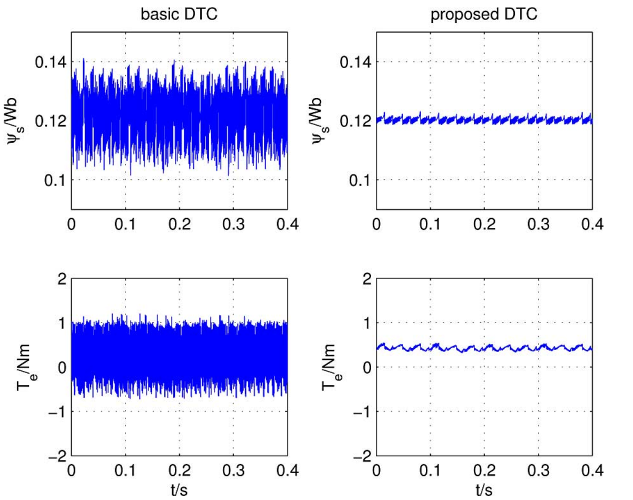

Fig. 22. Steady state response of stator flux and torque at 10% rated speed for conventional DTC and the proposed DTC.

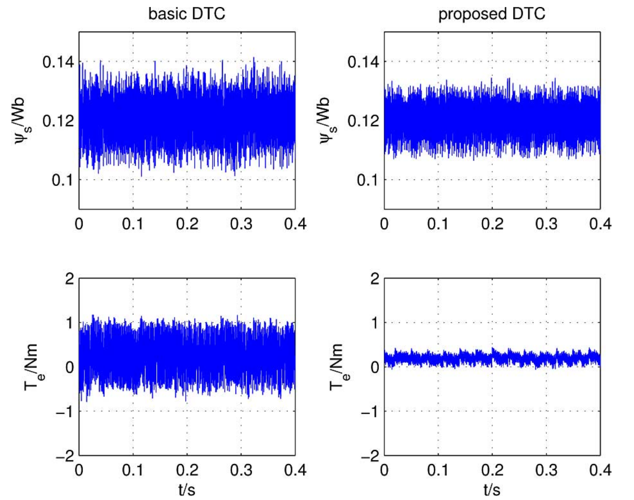

Fig. 23. Steady state response of stator flux and torque at 100% rated speed for conventional DTC and the proposed DTC.

against commutation frequency reduction, parameter mismatch, and sampling frequency change. The other methods have better performance in terms of torque ripple under ideal condition without one-step delay; their flux ripples are similar to that of conventional DTC if one-step delay is not compensated, which is in accordance with the conclusion in [16] for method III. Furthermore, they are also insensitive to commutation frequency reduction and parameter mismatch. The simulation results confirm the theoretical analysis in Section IV.

VII. Experimental Results

The experimental tests were carried out to validate the effectiveness of the proposed method. The whole diagram of system is the same as that in Fig. 6, in which the PMSM is fed by a two-level inverter using insulated gate bipolar transistors. The speed is obtained from a 2500-pulse incremental encoder. A dSpace DS1104 PPC/DSP control board is employed to implement the real-time algorithm coding using c language. The external load is applied using a programmable dynamometer controller DSP6000. Both torque and flux are estimated from the LPF-based voltage model with compensation. All experimental results are recorded using the ControlDesk interfaced with DS1104 and PC. The parameters of PMSM and control system are the same as listed in Table I. The one-step delay caused by the digital implementation in DSP is not compensated for the sake of simplicity. The commutation frequency reduction is implemented for the proposed method. The system sampling frequency is 10 kHz, and the constants for the proposed DTC are 2 Nm for C_T and 0.1 Wb for C_ψ, as introduced in Table I.

The steady-state performances at different speeds are first investigated. Figs. 22 and 23 present the steady response without load for conventional DTC and proposed DTC at 10% rated speed and 100% rated speed, respectively. From top to bottom, the curves illustrated in Fig. 22 and 23 are stator flux and electromagnetic torque. It is seen that in both low and high speed, there is significant reduction in torque and flux ripple, validating the effectiveness of the proposed method. The performance of

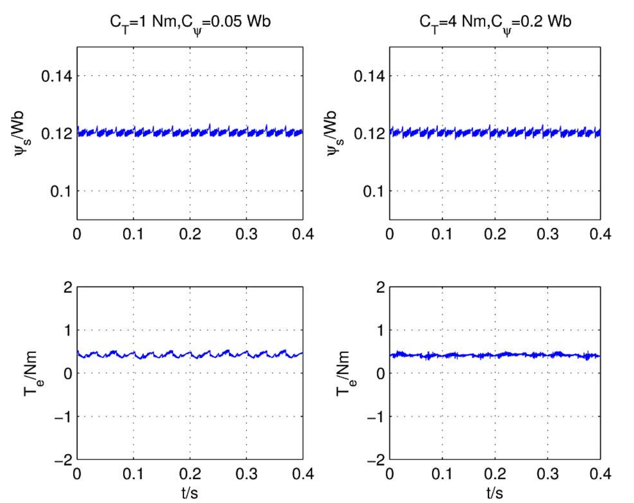

Fig. 24. Steady state response of stator flux and torque at 10% rated speed for the proposed DTC with different constant gains.

the proposed DTC at 10% rated speed with different constant gains for C_ψ and C_T is presented in Fig. 24. It is seen that there is little difference in the flux and torque ripples when compared to the result in Fig. 22, showing strong robustness against the variations of control parameters. Fig. 25 shows the torque and flux waveforms when switching from conventional DTC to proposed DTC at 25% rated speed without load. For conventional DTC, the ripples of torque and flux are almost constant, while the torque and flux ripples are increased with the speed in the proposed DTC. The steady stator flux locus at 10% and 100% rated speed are shown in Figs. 26 and 27. It is seen that the stator flux ripple in the proposed DTC is also reduced effectively, especially at low speed.

The comparisons of torque ripple, flux ripple, and commutation frequency for conventional DTC and proposed DTC are illustrated in Fig. 28. There is an average torque ripple reduction of 88.1% in the proposed DTC. The average flux ripple reduction is 67.4% and varies with the speed. At low speed

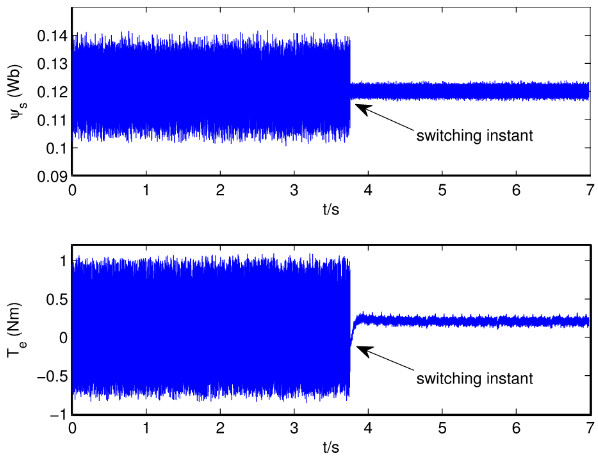

Fig. 25. Responses of stator flux and torque when switching from conventional DTC to the proposed DTC at 25% rated speed.

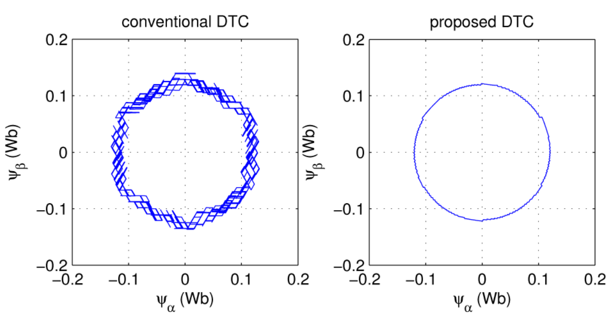

Fig. 26. Steady response of stator flux locus at 10% rated speed.

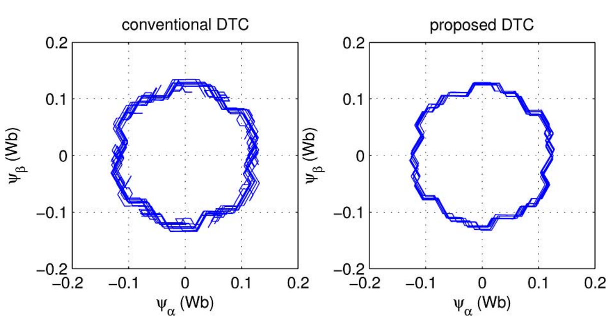

Fig. 27. Steady response of stator flux locus at 100% rated speed.

(200 r/m), the flux ripple is reduced significantly up to 84.8% and at high speed (2000 r/m) 39.4%. The torque ripple reduction varies slightly with the speed. The results under loaded condition are similar to that without load. The average commutation frequency is variable for conventional DTC, from 3.29 kHz at 10% rated speed to 2.15 kHz at 100% rated speed. For the proposed DTC, the average commutation frequency does not vary much, from 4.17 kHz at 10% rated speed to 4.85 kHz at 100% rated speed. The experimental results are in accordance with the simulation results shown in Table V.

Figs. 29 and 30 show the start-up response without load from standstill to rated speed for conventional DTC and proposed DTC, respectively. By introducing antiwindup in the PI controller, the motor speed accelerates to the nominal speed quickly

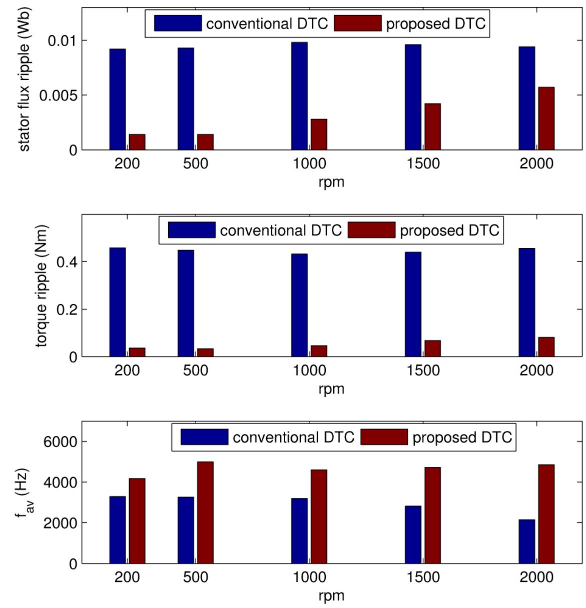

Fig. 28. Comparisons of flux ripple, torque ripple, and commutation frequency for conventional DTC and proposed DTC.

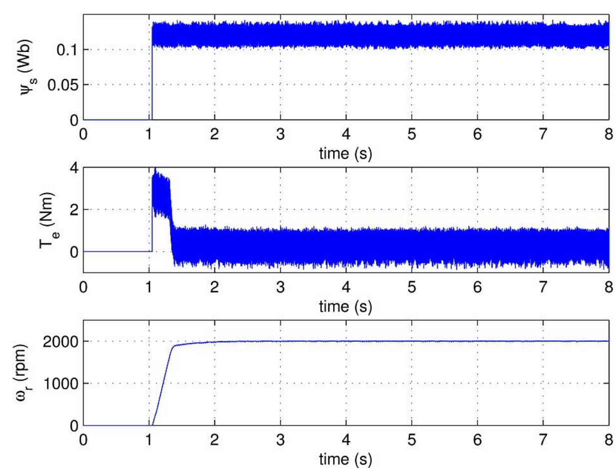

Fig. 29. Start-up responses of stator flux, torque, and speed from standstill to rated speed for conventional DTC.

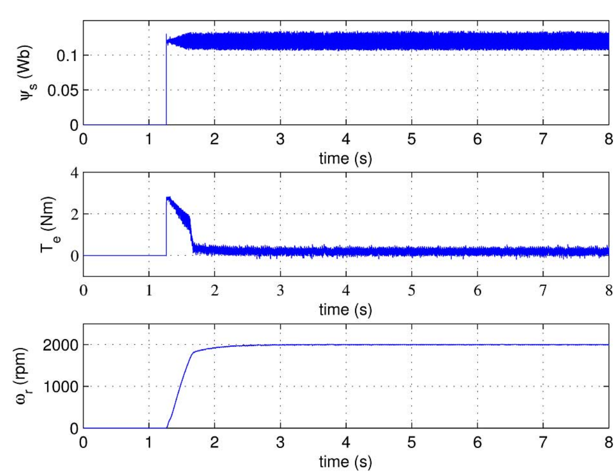

Fig. 30. Start-up responses of stator flux, torque, and speed from standstill to rated speed for the proposed DTC.

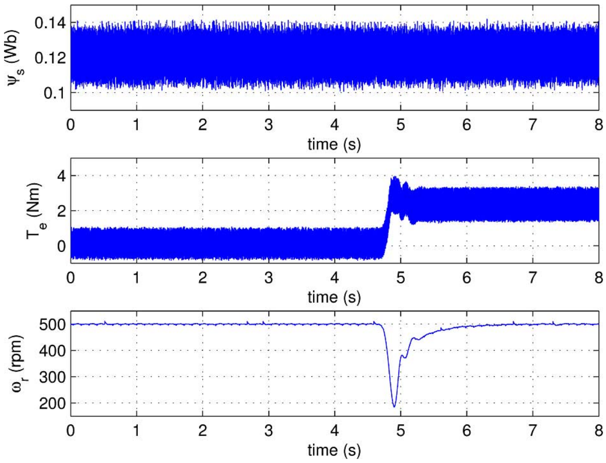

Fig. 31. Responses of stator flux, torque, and speed to external disturbance for conventional DTC.

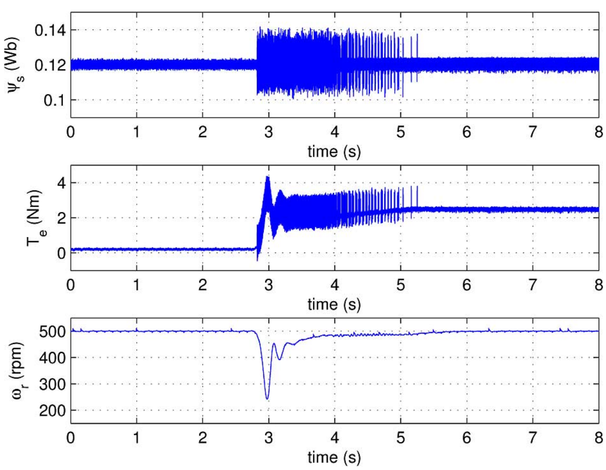

Fig. 32. Responses of stator flux, torque, and speed to external disturbance for the proposed DTC.

without overshoot. The dynamic response differences between proposed DTC and conventional DTC are insignificant, as illustrated in Fig. 30, hence maintaining the merit of quickness in conventional DTC.

The responses to external load disturbance of 2.5 Nm are illustrated in Figs. 31 and 32 for conventional DTC and proposed DTC, respectively. To enhance the dynamic performance and decrease the speed drop when external load is applied, the duty ratio calculation in proposed DTC is disabled when the motor speed error falls out of a certain range of 50 r/m, as shown in Fig. 32. The proposed DTC exhibits comparable dynamic response to conventional DTC. During the transient process, the active vector works during the whole period, i.e., $d = 1$, and the performance is similar to that in conventional DTC. When the motor speed error is less than 50 r/m, the duty ratio is reenabled and excellent steady performance is obtained.

VIII. Conclusion

A very simple yet effective method to obtain the duty ratio of the active vector is proposed in this paper, which can significantly reduce both torque and flux ripples in conventional DTC. By appropriately arranging the vector sequence during one cycle, the commutation frequency of the proposed DTC can be reduced up to 38.27% without degrading the steady performance. This fact can also be applied to other duty-based DTC methods, which has not been reported before. The proposed method only needs the information of torque and flux errors, while excellent steady performance is achieved. The dynamic response can be improved by disabling the duty calculation during transient process. The effectiveness of the proposed method is validated by simulation and experimental results and can be extended to other machines easily.

The performance of the proposed method is compared with three duty determination methods in detail using simulations, and it presents the merits of much easier implementation, lower flux ripple, and stronger robustness against one-step delay and parameter mismatch. However, if one-step delay is compensated, better performance in terms of torque ripple can be obtained by the analytical duty methods. Our first-stage work in this comparative study still lacks detailed experiments, and further effort is needed to confirm the theoretical analysis and simulations in this paper.

Acknowledgment

The authors would like to thank the anonymous reviewers for several helpful suggestions such as rational explanation of the proposed method and reconstruction in the description of the manuscript.

References

[1] D. Casadei, F. Profumo, G. Serra, and A. Tani, "FOC and DTC: Two viable schemes for induction motors torque control," *IEEE Trans. Power Electron.*, vol. 17, no. 5, pp. 779–787, Sep. 2002.

[2] I. Takahashi and T. Noguchi, "A new quick-response and high-efficiency control strategy of an induction motor," *IEEE Trans. Ind. Appl.*, vol. IA-22, no. 5, pp. 820–827, Sep. 1986.

[3] M. Depenbrock, "Direct self-control (DSC) of inverter-fed induction machine," *IEEE Trans. Power Electron.*, vol. 3, no. 4, pp. 420–429, Oct. 1988.

[4] G. S. Buja and M. P. Kazmierkowski, "Direct torque control of PWM inverter-fed AC motors—A survey," *IEEE Trans. Ind. Electron.*, vol. 51, no. 4, pp. 744–757, Aug. 2004.

[5] G. Foo and M. F. Rahman, "Sensorless direct torque and flux-controlled IPM synchronous motor drive at very low speed without signal injection," *IEEE Trans. Ind. Electron.*, vol. 57, no. 1, pp. 395–403, Jan. 2010.

[6] G.-D. Andreescu, C. Pitic, F. Blaabjerg, and I. Boldea, "Combined flux observer with signal injection enhancement for wide speed range sensorless direct torque control of IPMSM drives," *IEEE Trans. Energy Convers.*, vol. 23, no. 2, pp. 393–402, Jun. 2008.

[7] V. Ambrozic, G. S. Buja, and R. Menis, "Band-constrained technique for direct torque control of induction motor," *IEEE Trans. Ind. Electron.*, vol. 51, no. 4, pp. 776–784, Aug. 2004.

[8] C. Lascu and A. Trzynadlowski, "Combining the principles of sliding mode, direct torque control, and space-vector modulation in a high-performance sensorless ac drive," *IEEE Trans. Ind. Appl.*, vol. 40, no. 1, pp. 170–177, Jan./Feb. 2004.

[9] Y.-S. Lai and J.-H. Chen, "A new approach to direct torque control of induction motor drives for constant inverter switching frequency and torque ripple reduction," *IEEE Trans. Energy Convers.*, vol. 16, no. 3, pp. 220–227, Sep. 2001.

[10] B. Kenny and R. Lorenz, "Stator- and rotor-flux-based deadbeat direct torque control of induction machines," in *IEEE Trans. Ind. Appl.*, vol. 39, no. 4, pp. 1093–1101, Jul./Aug. 2003.

[11] M. Mengoni, L. Zarri, A. Tani, G. Serra, and D. Casadei, "Stator flux vector control of induction motor drive in the field weakening region," *IEEE Trans. Power Electron.*, vol. 23, no. 2, pp. 941–949, Mar. 2008.

[12] M. Jemli, H. Ben Azza, M. Boussak, and M. Gossa, "Sensorless indirect stator field orientation speed control for single-phase induction motor drive," *IEEE Trans. Power Electron.*, vol. 24, no. 6, pp. 1618–1627, Jun. 2009.

[13] J. Beerten, J. Verveckken, and J. Driesen, "Predictive direct torque control for flux and torque ripple reduction," *IEEE Trans. Ind. Electron.*, vol. 57, no. 1, pp. 404–412, Jan. 2010.

[14] S. Kouro, R. Bernal, H. Miranda, C. Silva, and J. Rodriguez, "High-performance torque and flux control for multilevel inverter fed induction motors," *IEEE Trans. Power Electron.*, vol. 22, no. 6, pp. 2116–2123, Nov. 2007.

[15] Y. Zhang, J. Zhu, Y. Guo, W. Xu, Y. Wang, and Z. Zhao, "A sensorless DTC strategy of induction motor fed by three-level inverter based on discrete space vector modulation," in *Proc. Australasian Univ. Power Eng. Conf. (AUPEC 2009)*, pp. 1–6..

[16] J.-K. Kang and S.-K. Sul, "New direct torque control of induction motor for minimum torque ripple and constant switching frequency," *IEEE Trans. Ind. Appl.*, vol. 35, no. 5, pp. 1076–1082, Sep./Oct. 1999.

[17] K.-B. Lee, J.-H. Song, I. Choy, and J.-Y. Yoo, "Torque ripple reduction in DTC of induction motor driven by three-level inverter with low switching frequency," *IEEE Trans. Power Electron.*, vol. 17, no. 2, pp. 255–264, 2002.

[18] E. Flach, R. Hoffmann, and P. Mutschler, "Direct mean torque control of an induction motor," in *Proc. EPE*, 1997, vol. 3, pp. 672–677.

[19] L. Romeral, A. Arias, E. Aldabas, and M. Jayne, "Novel direct torque control (DTC) scheme with fuzzy adaptive torque-ripple reduction," *IEEE Trans. Ind. Electron.*, vol. 50, no. 3, pp. 487–492, Jun. 2003.

[20] S. Kouro, P. Cortes, R. Vargas, U. Ammann, and J. Rodriguez, "Model predictive control—A simple and powerful method to control power converters," *IEEE Trans. Ind. Electron.*, vol. 56, no. 6, pp. 1826–1838, Jun. 2009.

[21] T. Geyer, G. Papafotiou, and M. Morari, "Model predictive direct torque control Part I: Concept, algorithm, and analysis," *IEEE Trans. Ind. Electron.*, vol. 56, no. 6, pp. 1894–1905, Jun. 2009.

[22] K. Drobnic, M. Nemec, D. Nedeljkovic, and V. Ambrozic, "Predictive direct control applied to AC drives and active power filter," *IEEE Trans. Ind. Electron.*, vol. 56, no. 6, pp. 1884 –1893, Jun. 2009.

[23] H. Miranda, P. Cortes, J. Yuz, and J. Rodriguez, "Predictive torque control of induction machines based on state-space models," *IEEE Trans. Ind. Electron.*, vol. 56, no. 6, pp. 1916–1924, Jun. 2009.

[24] F. Morel, X. Lin-Shi, J.-M. Retif, B. Allard, and C. Buttay, "A comparative study of predictive current control schemes for a permanent-magnet synchronous machine drive," *IEEE Trans. Ind. Electron.*, vol. 56, no. 7, pp. 2715–2728, Jul. 2009.

[25] J. Restrepo, J. Aller, J. Viola, A. Bueno, and T. Habetler, "Optimum space vector computation technique for direct power control," *IEEE Trans. Power Electron.*, vol. 24, no. 6, pp. 1637–1645, Jun. 2009.

[26] M. W. Naouar, A. Ammar Naassani, E. Monmasson, and I. Slama Belkhodja, "FPGA-based predictive current controller for synchronous machine speed drive," *IEEE Trans. Power Electron.*, vol. 23, no. 4, pp. 2115–2126, Jul. 2008.

[27] R. Morales-Caporal and M. Pacas, "Encoderless predictive direct torque control for synchronous reluctance machines at very low and zero speed," *IEEE Trans. Ind. Electron.*, vol. 55, no. 12, pp. 4408–4416, Dec. 2008.

[28] G. Abad, M. A. Rodriguez, and J. Poza, "Two-level VSC based predictive direct torque control of the doubly fed induction machine with reduced torque and flux ripples at low constant switching frequency," *IEEE Trans. Power Electron.*, vol. 23, no. 3, pp. 1050–1061, May 2008.

[29] K. D. Hurst, T. G. Habetler, G. Griva, and F. Profumo, "Zero-speed tacholess IM torque control: Simply a matter of stator voltage integration," *IEEE Trans. Ind. Appl.*, vol. 34, no. 4, pp. 790–795, Jul. 1998.

[30] J. Hu and B. Wu, "New integration algorithms for estimating motor flux over a wide speed range," *IEEE Trans. Power Electron.*, vol. 13, no. 5, pp. 969–977, Sep. 1998.

[31] B. K. Bose and N. R. Patel, "A programmable cascaded low-pass filter-based flux synthesis for a stator flux-oriented vector-controlled induction motor drive," *IEEE Trans. Ind. Electron.*, vol. 44, no. 1, pp. 140–143, Feb. 1997.

[32] T.-W. Chun, M.-K. Choi, and B. K. Bose, "A novel startup scheme of stator-flux-oriented vector-controlled induction motor drive without torque jerk," *IEEE Trans. Ind. Appl.*, vol. 39, no. 3, pp. 776–782, May 2003.

[33] M. Hinkkanen and J. Luomi, "Modified integrator for voltage model flux estimation of induction motors," *IEEE Trans. Ind. Electron.*, vol. 50, no. 4, pp. 818–820, Aug. 2003.

[34] Y. Zhang, Z. Zhao, T. Lu, L. Yuan, W. Xu, and J. Zhu, "A comparative study of Luenberger observer, sliding mode observer and extended Kalman filter for sensorless vector control of induction motor drives," in *Proc. IEEE Energy Convers. Congr. Expo. (ECCE 2009)*, pp. 2466–2473.

[35] T. Habetler, F. Profumo, M. Pastorelli, and L. Tolbert, "Direct torque control of induction machines using space vector modulation," *IEEE Trans. Ind. Appl.*, vol. 28, no. 5, pp. 1045–1053, Sep./Oct. 1992.

[36] M. Pacas and J. Weber, "Predictive direct torque control for the PM synchronous machine," *IEEE Trans. Ind. Electron.*, vol. 52, no. 5, pp. 1350–1356, Oct. 2005.

[37] L. Zhong, M. Rahman, W. Hu, and K. Lim, "Analysis of direct torque control in permanent magnet synchronous motor drives," *IEEE Trans. Power Electron.*, vol. 12, no. 3, pp. 528–536, May 1997.

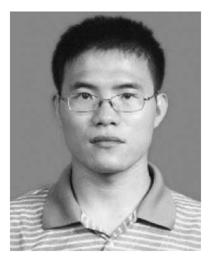

Yongchang Zhang (M'10) received the B.E. degree from Chongqing University, Chongqing, China, in 2004, and the Ph.D. degree from Tsinghua University, Beijing, China, in 2009, both in electrical engineering.

He is currently a Postdoctoral Fellow at the University of Technology, Sydney, Australia. His research interests include sensorless and high performance control of ac motor drives, control of multilevel converters, optimal pulsewidth modulation, and advanced digital control with real-time implementation.

Jianguo Zhu (S'93–M'96–SM'03) received the B.E. degree from Jiangsu Institute of Technology, Nanjing, China, in 1982, the M.E. degree from Shanghai University of Technology, Shanghai, China, in 1987, and the Ph.D. degree from the University of Technology, Sydney (UTS), Australia, in 1995.

He is currently a Professor of electrical engineering and the Head of the School of Electrical, Mechanical and Mechatronic Systems, UTS. His research interests include electromagnetics, magnetic properties of materials, electrical machines and drives, power electronics, and renewable energy systems.